

The Phenomenology of Strings and Clusters in the 3- d Ising Model

Vladimir S. Dotsenko[*], Marco Picco and Paul Windey

LPTHE[†]

Université Pierre et Marie Curie, Bte 126, 4 Place Jussieu
75252 Paris CEDEX 05, FRANCE

Geoffrey Harris and Enzo Marinari[‡]

Physics Department and NPAC, Syracuse University
Syracuse, NY 13244, USA

Emil Martinec

Enrico Fermi Institute and Department of Physics, University of Chicago
Chicago, IL 60637, USA

November 1993

hep-th/9401129
SU-HEP-4241-563
PAR-LPTHE 93/59

Abstract

We examine the geometrical and topological properties of surfaces surrounding clusters in the 3- d Ising model. For geometrical clusters at the percolation temperature and Fortuin–Kasteleyn clusters at T_c , the number of surfaces of genus g and area A behaves as $A^{x(g)} e^{-\mu(g)A}$, with x approximately linear in g and μ constant. We observe that cross-sections of spin domain boundaries at T_c decompose into a distribution $N(l)$ of loops of length l that scales as $l^{-\tau}$ with $\tau \sim 2.2$. We address the prospects for a string-theoretic description of cluster boundaries.

1 Introduction

One of the major successes of 20th century physics has been the expression of the critical behavior of a variety of theories of nature in terms of sums over decorated, fluctuating paths. It has thus also been hoped that higher dimensional analogues, theories of fluctuating membranes, also play a fundamental role in characterizing the physics of critical phenomena. In particular, significant effort has been invested in recasting one of the simpler models of phase transitions, the $3-d$ Ising model, as a theory of strings [1]. These attempts have been stymied by the difficulty in taking the continuum limit of formal sums over lattice surfaces.

In fact, sums over lattice surfaces, built from e.g. plaquettes or polygons, generically fail to lead to a well-defined continuum theory of surfaces. An exception to this rule occurs when the surface discretizations are embedded in $d \leq 1$. In this case, one can exactly solve a large class of toy lattice models which lead to sensible continuum ‘bosonic’ string theories (at least perturbatively) [2]. Numerically, it is observed that the $d > 1$ versions of these lattice models suffer a ‘fingering instability’; the embedded surfaces, for instance are composed of spikes with thickness of the order of the cutoff. It is suspected that the polygonal discretization of the worldsheet (for large volumes) is configured in a polymer-like structure, so that these theories cannot be realized as sums over surfaces in the continuum limit. This instability is anticipated theoretically, since the mass-squared of the dressed identity operator of the bosonic string becomes negative above $d = 1$, presumably generating an uncontrolled cascade of states that tear the worldsheet apart[3].

In the continuum limit, we know how to evade these problems in special cases through the implementation of supersymmetry and the GSO projection. This additional structure, however, leads to fundamental difficulties in discretizing these theories. In principle, one might hope to somehow guess an appropriate continuum string theory and then show that it embodies the critical behavior of a lattice theory, such as the $3-d$ Ising model. The prospects for success through such an approach seem rather poor at this time.

Given this state of affairs, we have turned to a more phenomenological approach, in which we attempt to generate ‘physical’ random surfaces in a particular model and then examine their topological and geometrical properties. We thus have chosen to look at the structure of domain boundaries in the $3-d$ Ising model. The phenomenology of these self-avoiding cluster bound-

aries is interesting in its own right, since it describes a large universality class of behavior that is expressed frequently and quite precisely by nature. We also might hope that our observations may be useful in gauging the prospects of success of a string–theoretic description. The Ising model has been employed previously as a means to generate random lattice surfaces¹; see for instance, the work of David [4], Huse and Leibler [5], Karowski and Thun and Schrader [6]. In a sense, this work extends these studies by looking for new features of the geometry of these lattice surfaces; we also consider boundaries of Fortuin–Kasteleyn clusters as well as ‘geometrical’ spin domains. Much of our analysis consists of a measurement of the distribution of surfaces as a function of their area A and genus g , $N_g(A)$ ². We shall determine the functional form of $N_g(A)$. We also perform block spin measurements of the genus, to determine if a condensation of handles is present on cluster boundaries at all scales. These cluster boundaries are strongly coupled and thus it appears cannot be directly characterized by perturbative string theory. We see that, however, boundaries of spin domains at the Curie temperature are not just strongly–coupled versions of the branched polymer–like objects that attempts to build ‘bosonic’ random surfaces typically generate. They instead exhibit a richer fractal structure, albeit one not characteristic of surfaces. We show that they obey a new scaling law that describes the distribution $N(l)$ of lengths l of loops that compose cross–sections of cluster boundaries.

2 Ising Clusters and Surfaces

We shall begin by summarizing the basic physical properties of the cluster boundaries that we have analyzed. To a first approximation, a 2–dimensional membrane of area A and curvature matrix K will exact an energy cost [5, 8]

$$H = \mu A + \lambda \int (\text{Tr}K)^2 + \kappa \int \text{Det}K; \quad (1)$$

μ is the bare surface tension, λ is referred to as the bending rigidity and κ couples to the Euler character of the surface. In the regime which char-

¹Through the use the phrase ‘lattice surface’ rather than ‘surface’, we indicate that these objects should *not* be necessarily inferred to be real surfaces in the continuum limit.

²The mean genus per Ising configuration is measured in references [6]. A determination of genus as a function of area in an Ising system with anti–periodic boundary conditions have also appeared recently [7].

acterizes random surfaces, the surface tension must be sufficiently small to allow significant thermal fluctuations. Note that the above action does not capture the entire dynamics; it is essential also to keep in mind that Ising cluster boundaries are naturally self-avoiding. We first consider surfaces in the dual lattice that bound ‘geometrical clusters’ formed from sets of adjacent identical spins. In this case, the Ising dynamics generates an energy penalty proportional to the boundary area; λ_{bare} and $\kappa_{bare} = 0$. The bare surface tension is tuned by the Ising temperature. To put this model in perspective, we note that for real vesicles, for instance, the couplings λ and κ can be quite large; λ ranging from about kT to $100kT$ have been measured [8]. The bending rigidity may be irrelevant in the continuum limit, however. The string coupling ³ is equal to $\exp(-\kappa)$. Through blocking spins, we make an estimate of the renormalization group behavior of κ . Unless κ effectively becomes large in the infrared, the cluster boundaries will fail to admit a surface description in the continuum limit.

The geometrical clusters and their boundaries are *not* present at all scales at the Curie temperature. Instead, for temperatures somewhat below T_c and all temperatures above T_c two huge geometrical clusters comprise a finite fraction of the entire lattice volume. These clusters percolate, that is, they wrap around the entire lattice (we shall consider periodic boundary conditions). Otherwise, the lattice only contains very small clusters that are the size of a few lattice spacings; there are no intermediate size clusters. We can understand this behavior by considering the $T \rightarrow \infty$ behavior of these clusters. Two percolated clusters span the lattice even at infinite temperature, where clusters are smaller than at T_c . At $T = \infty$, the spins are distributed randomly with spin up with probability 50%; the problem of constructing clusters from these spins then reduces to pure site percolation with $p = 1/2$. Pure site (or bond) percolation describes the properties of clusters built by identifying adjacent colored bonds (sites), which are colored randomly with probability p . Above a critical value $p = p_c$, the largest of these clusters percolates through the lattice[9]. For the cubic lattice, it is known that an infinite cluster will be generated (in the thermodynamic limit) at $p_c \sim .311$. Thus, the fact that the geometrical clusters have percolated in the high-temperature regime and at the Curie point is essentially a consequence of the connectivity of 3- d lattices.

³We ignore distinctions between intrinsic and extrinsic metrics.

At very low temperatures, however, there are few reversed (minority) spins in the Ising model; these form a few small clusters. As the density of minority spins increases, the clusters become bigger until the largest cluster percolates at some temperature $T_p < T_c$. It has been suggested (see [10] and [5]) that since this minority spin percolation appears to be due to an increase in the concentration of minority spins and not to any long-distance Ising dynamics, that this transition is in the same universality class as pure (bond or site) percolation. We emphasize that the scaling of minority clusters should not correspond to any non-analyticity in the thermodynamic behavior of the Ising model; it should essentially be a ‘geometric effect’.

There is another type of cluster, introduced by Fortuin and Kasteleyn [11, 12], that does proliferate over all length scales at the Curie point. These FK clusters consist of sets of bonded spins; one draws these bonds between adjacent same-sign spins with a temperature dependent probability $p = 1 - \exp(-2\beta)$. Note that the geometrical clusters are built by a similar procedure, using instead $p = 1$. FK clusters arise naturally in the reformulation of the Ising model as a percolating bond/spin model [13]. For the Ising partition function can be recast as a sum over occupied and unoccupied bonds with partition function

$$Z = \sum_{\text{bonds}} p^b (1-p)^{(N_b-b)} 2^{N_c} \quad (2)$$

where $p = 1 - \exp(-2\beta)$, N_b denotes the number of bonds in the entire lattice in which b bonds are occupied and N_c equals the number of clusters that these occupied bonds form. When the factor 2^{N_c} is replaced by q^{N_c} , then (2) is the partition function for the q -state Potts model. If we assign a spin to each bond so that all bonds in the same cluster have the same spin, then the factor of q^{N_c} just comes from a sum over spin states. The above partition function can then be viewed as a sum over FK clusters. Using this construction, one can show that the spin-spin correlator in the original Ising model is equal to the pair connectedness function of FK clusters,

$$\langle \sigma(x)\sigma(y) \rangle = \langle \delta_{C_x, C_y} \rangle, \quad (3)$$

which equals the probability that points x and y belong to the same FK cluster [14]. It then follows that for $T \geq T_c$, the mean volume of the FK clusters is proportional to the susceptibility of the Ising model, so that indeed FK

clusters only just start to percolate at the Curie point. Additionally, the relation (3) also implies that the spatial extent of the FK clusters is proportional to the correlation length of the Ising model. Furthermore, scaling arguments [15] demonstrate that at T_c , the volume distribution of FK clusters obeys

$$N(V_{cl}) \simeq V_{cl}^{-\tau}, \quad \tau = 2 + \frac{1}{\delta}, \quad (4)$$

where δ denotes the magnetic exponent of the Ising model ($M \simeq B^{1/\delta}$). Thus we see that FK clusters, unlike the geometrical clusters previously discussed, directly encode the critical properties of the Ising model. Indeed, we are necessarily led to study FK clusters in order to measure scaling laws that characterize cluster boundaries of the scale of the Ising correlation length, i.e. boundaries that scale at the Curie point. On the other hand, geometrical cluster boundaries contribute an energy penalty proportional to their individual area; the lattice surface dynamics of FK cluster boundaries, however, cannot be likewise described by a similar physical rule.

In 2–dimensions both the FK clusters and the geometrical clusters percolate at the Curie temperature. The critical properties of these clusters differ, however, since the scaling of geometrical clusters is partially determined by the ‘percolative’ properties of two–dimensional lattices. These effects are in some sense removed through the FK construction.

3 The Simulation

We now proceed to outline the techniques used in our Monte Carlo simulations. We analyzed data from lattices of size ranging from $L = 32$ to $L = 150$, using about six months of time on RISC workstations. Spin updates were implemented through the efficient Swendsen–Wang algorithm [16]: FK clusters for each lattice configuration are first constructed, then the spins composing each cluster are (all) assigned a new random spin value. We determined our statistical uncertainties via the jackknife technique and extracted exponents through linear least–squared fits. Statistical errors for these exponents were also obtained by using jackknife when fitting. Generally, systematic corrections to scaling and finite-size effects are much larger than our statistical errors.

The main technical difficulty that we encountered was the measurement of the Euler character, equal to $V - E + F$ for a dual surface with V vertices,

E edges and F faces. On the simple cubic (SC) lattice, the construction of the dual surface is ambiguous for configurations in which 4 plaquettes intersect along the same link, for instance. We found that we could define a consistent set of rules, which we shall discuss in [17], that resolved these ambiguities. These rules are certainly not unique; one would hope that their implementation essentially serves as a regularization that does not affect long-distance scaling laws.

In two dimensions, one can avoid ambiguous intersections on the dual lattice by considering Ising spins on the triangular lattice. Its dual (the honeycomb lattice) is trivalent and thus Ising spin domains will not be enclosed by self-intersecting paths. This fortuitous situation generalizes to three-dimensions for the Ising model on a body centered cubic (BCC) lattice in which the vertices at the center of each cube are also connected to those in the centers of neighboring cubes. More explicitly, we coupled with equal strength both the 6 nearest and 8 next-nearest Ising spins so that only three plaquettes of the dual lattice meet along a dual link. Since surfaces built dual to this lattice are also naturally self-avoiding, computing the genus is trivial. A depiction of the Wigner-Seitz cell of this lattice (composed of plaquettes in the dual lattice) appears in figure 1.

Estimating the appropriate critical temperatures also required considerable effort. To find the percolation temperature β_p we used the method discussed by Kirkpatrick [18] in which one measures the fraction f of configurations containing clusters that span the lattice. One plots f versus β for different lattice sizes L ; β_p corresponds to the intersection of these curves for different L . On the BCC lattice, we checked this by also determining the temperature at which the mean cluster size scales as a power law in L . From this analysis, we obtained $\beta_p = .0959$ on the BCC lattice and $\beta_p = .232$ on the SC lattice. The value of β_c on the SC lattice has been previously determined to be about .221651 [19]; we also found that $\beta_c \sim .0858$ on the BCC lattice.

4 Results

We now present data from our simulations on both the simple cubic and BCC lattices. We have examined boundaries of FK clusters at T_c , surfaces bounding minority spin domains at T_p and geometrical clusters at T_c . In

[17], a more comprehensive discussion of our data will appear, including also results from simulations of the 2- d Ising model and pure bond percolation in 3 dimensions. A more concise summary of some of these results has been presented in [20].

4.1 Cluster Properties

We begin by discussing a few of the properties of the clusters. Most of the new material, pertaining to the topology of the cluster boundaries, appears in the following sub-sections.

For FK clusters at T_c and minority clusters at T_p , we verified the scaling given in (4). This is shown, for example, in figure 2 for FK clusters on an $L = 64$ SC lattice. We observe good power law scaling over a large region of V_{cl} . The bump in $N(V_{cl})$ and subsequent steep drop-off describes the distribution of clusters that span a significant fraction of the lattice and are thus subject to large finite-size effects. In principle, by carefully determining $\tau = 2 + 1/\delta$, one might hope to provide concrete numerical evidence for the very reasonable hypothesis that the transition at T_p is in the universality class of pure percolation. In practice, this is quite difficult. The value of the magnetic exponent δ in the 3- d Ising model (as determined through renormalization group methods, for instance) yields the prediction $\tau_{\text{FK}} = 2.207(1)$ [21]. The value of τ for pure percolation that one would infer from recent series expansions is $\tau = 2.189(5)$ [9], which is not so different from the FK value.

In fact, the power law fits to $N(V_{cl})$ are not very precise, due to large finite volume effects and corrections to scaling. The values we extract from these plots are $\tau_{\text{FK}} = 2.25(10)$ (this has been measured by Wang [15]) and $\tau_{\text{geo}} = 2.10(5)$ on the largest ($L = 64$ and 100) lattices that we considered. This is a rather poor way to measure these exponents; much more accurate estimates can be obtained through finite-size scaling fits of the mean cluster size as a function of lattice size L . The mean cluster size scales as $L^{\gamma/\nu}$; standard scaling relations and (4) give $\tau = (3 + \gamma/\nu d)/(1 + \gamma/\nu d)$ ($d = 3$). Using this technique, we measured $\tau_{\text{FK}} = 2.207(3)$ on the SC lattice and $\tau_{\text{geo}} = 2.202(3)$ on the BCC lattice. The error on τ_{geo} is in fact probably several times larger than quoted above, due to uncertainties in locating the critical temperature. This measurement of τ_{FK} agrees perfectly with previous values; the measurement of τ_{geo} is not accurate enough to distinguish likely

pure percolation behavior from that of percolation of FK clusters.

We measured the number of sites on the boundary of each cluster, A_{cl} . A plot of $\ln(V_{cl}/A_{cl})$ vs. $\ln(V_{cl})$ for FK clusters on an $L = 64$ BCC lattice appears in figure 3. We see that for very small volumes, the lattice regularization constrains V_{cl} to equal A_{cl} and for intermediate volumes, there is a small deviation from linear scaling (as some interior sites begin to appear). The plateau that appears around $V_{cl} = 3000$ indicates the onset of scaling regime where $A_{cl} \propto V_{cl}$. The growth just at the end of the plot is due to the largest cluster, which wraps around the lattice and merges with itself to form extra interior points. This plateau indicates that the lattice surfaces are not smooth and may be configured as polymer-like networks.

This behavior is not surprising. The observed proportionality of V_{cl} and A_{cl} is well-known in the context of pure percolation in 2 and 3 dimensions [9]. Bonds (or sites) are deleted with a fixed probability in percolation. This implies that holes should be distributed homogeneously with finite measure on percolation clusters; i.e. the boundary length should be proportional to the enclosed volume. Note that FK clusters are constructed by performing percolation on geometrical clusters, so this argument should definitely apply in the FK case. We also found $A_{cl} \propto V_{cl}$ for geometrical clusters at T_p ; this observation is consistent with the intuition that the T_p transition is that of pure percolation.

4.2 Genus Distribution

We now turn to an analysis of the distribution of handles on cluster boundaries. If these boundaries form tangled networks, then the following essentially characterizes the statistics of closed loops in these networks. In the simplest scenario, one might assume that the handles are uncorrelated. It would then follow that $N_g(A)$ asymptotically obeys the Poisson distribution $N_g(A) = \kappa_g(\mu A)^g e^{-\mu A}$, with $\kappa_g \propto 1/g!$. The probability per plaquette of growing a handle is then μ .

We first present a sample of fits to $N_g(A)$ for FK cluster boundaries on the BCC lattice for $L = 64$. In figure 4, we present our data for genus 2 along with a best fit to the functional form

$$N_g(A) = C_g A^{x(g)} e^{-\mu(g)A} . \quad (5)$$

$N_2(A)$ is peaked near $A = 250$, and the fit is perfect apart from the very small

area region, where we expect corrections to scaling to be large. Likewise, the power law plus exponential fit is superb for genus 5 as indicated in figure 5. We find that this functional form fits our data very well for $g \geq 2$ up to about $g = 20$ where our statistics become poor. If we assume that the ansatz (5) holds, then it follows that

$$\mu = \mu_{eff} \equiv \frac{\langle A \rangle}{(\langle A^2 \rangle - \langle A \rangle^2)} \quad (6)$$

and

$$x(g) = x_{eff} \equiv \frac{\langle A \rangle^2}{(\langle A^2 \rangle - \langle A \rangle^2)} - 1 . \quad (7)$$

We measured these moments and found that indeed μ_{eff} and x_{eff} agreed very well with the values extracted directly from fits to (5). The value $\mu_{eff}^{-1} = 114 \pm 3$ as depicted in figure 6 is proportional to the average surface area (in lattice units) per handle and is independent of genus for $g > 2$. In figure 7 we show the genus dependence of the exponent x , extracted both from moments of the area distribution and from the direct fits. After a transient region for small genus ($g = 0-4$) we find almost linear behavior in the region $g = 5-15$ with a slope of 1.25 ± 0.1 .

The results for FK clusters on the SC lattice are quite similar, though not as clean. We first show the behavior of $N_1(A)$ for $L = 64$ in figure 8. Clearly, here the fit does not work, though one does expect large deviations from asymptotic scaling for surfaces in the range depicted. The fit for genus 5 (figure 9), however, is quite good, although small systematic discrepancies are still notable. Perhaps the regularization needed to define genus in the SC case is partially responsible for these deviations. Again, for the SC lattice, we find that μ appears to be independent of g , though we observe a very small systematic drift. The plot of $x(g)$ vs. g exhibits more curvature than in the BCC case, but the slope in the genus 5 – 15 region again is about 1.25.

The deviation of 1.25 from 1 at first glance suggests the presence of significant deviations from Poisson distributed behavior. This may be due, however, to systematic deviations from continuum behavior due to lattice artifacts. The magnitude of these systematic errors is illustrated by the measurement of the dependence of the mean area on genus. If we assume the ansatz (5) then we would predict that the mean dual surface area A should

increase linearly with genus, obeying

$$\langle A(g) \rangle = \frac{x(g) + 1}{\mu(g)}. \quad (8)$$

For FK clusters on the BCC lattice, however, we see by fitting $\ln \langle A \rangle$ to $\ln g$ in the small genus regime that $\langle A \rangle$ is not precisely linear in g ; in fact it scales roughly as $g^{.85}$. Note that such a scaling law could not hold asymptotically for large lattices and large areas, since it would imply that surfaces would have more handles than plaquettes. Indeed this effective exponent slowly increases with genus (to roughly .90 at $g = 50$). Thus we observe systematic deviations (of order 15%) of genus dependent exponents from their asymptotic values. This also indicates that the apparent linearity that we observed in $x(g)$ is somewhat deceiving; presumably deviations from linearity would be more apparent if our statistics were better and we could directly fit somewhat higher values of g . The slope of $x(g)$ should decrease with greater g , so that the above estimate of the slope (1.25) may be too large.

The genus behavior of geometrical clusters at T_p is qualitatively quite similar to that of the FK case just discussed. We show fits to $N_2(A)$ and $N_5(A)$ on an $L = 60$ lattice in figures 10 and 11. There are large deviations in the fit for genus 2; for genus 4 and larger, however, the fits are nearly perfect. Again, μ is approximately independent of g , though (from figure 12) we observe transient behavior that is very significant up to genus 10. Again, x is approximately linear in g (as shown in figure 13), with a slope considerably lower than in the FK case; $dx/dg \sim 0.7 \pm 0.1$ in the range $g = 3 - 40$ for Ising minority spin percolation. The same caution as before applies to these slope values; systematic errors could still be quite large, so the actual value of .7 for the slope is not so trustworthy. In this case, potential deviations from asymptotic scaling reveal themselves most clearly through the transient behavior of μ .

From this analysis, we can conclude that the genus distribution of FK cluster boundaries at T_c and geometrical cluster boundaries at T_p is described by the functional form (5), with $x(g)$ approximately linear in g and μ constant. The lattices considered, however, are too small to characterize the behavior of x more precisely.

4.3 Loop Scaling and Blocked Spins

In this section, we will solely be concerned with the structure of boundaries of geometrical clusters as T is increased beyond T_p , particularly to $T = T_c$. Recall that for $T > T_p$, two percolated clusters of opposite sign will span the lattice. For T not so close to T_c , we expect that the characteristics of the Ising interaction will not influence the large-scale structure of these percolating clusters. The percolating clusters (assuming the transition at T_p is indeed in the universality class of pure percolation) should then be described by the ‘links, nodes and blobs’ picture developed for the infinite clusters of pure percolation in dimensions below $d_c = 6$ [9, 22]. In this description, the links form the thin backbones of the cluster; they are connected together at the nodes which occur roughly every percolation correlation length ξ . Most of the volume of the cluster consists of dangling ends emanating from the backbones. The backbones do not consist merely of one segment; they contain multiply-connected paths (which close to form the handles that we measure) that form blobs with diameter up to size ξ .

A cross section of the boundaries of these networks of tangled thin tubes would presumably be composed of a set of small lattice-sized loops. To check this, we examined the phase boundaries between up and down spins on planar slices of both the SC and BCC lattices. In figure 14, we show a log-log plot of $N(l)$, the number of loops of length l , versus l taken at the percolation temperature $\beta_p = .232$ on the SC lattice. The curve exhibits a sharp drop-off, indicating indeed that these slices contain only small loops. As we dial the temperature up towards T_c , we find that larger loops begin to appear in the slices. In fact, at T_c , we find loops at all scales; $N(l) \sim l^{-\tau}$! This scaling is depicted in the log-log plot in figure 15. As in figure 2, we observe a small bump at the end of the distribution followed by a rapid drop-off. These deviations from scaling are again due to the influence of the finite-size of the lattice on the largest loops. All of the largest loops must bound the two percolating clusters, since there are no intermediate size geometrical clusters at T_c . The loops themselves have a non-trivial fractal structure; we determined that the number of sites enclosed within a loop of length l scales as $A(l) \sim l^{\delta'}$.

From these measurements, we estimated that $\tau' = 2.06(3)$ and $\delta' = 1.20(1)$. These values are probably not very accurate, however. As in the determination of τ from the behavior of $N(V_{cl})$, corrections to scaling and

finite-size effects are a source of large systematic errors. These systematic effects were only of order 1 – 2% for δ ; thus we suspect that our estimate of δ' is considerably better than that of τ' . Carrying out these measurements also required a resolution of certain ambiguities. In particular, since the boundaries of domains self-intersect on slices of the cubic lattice, we had to pick a prescription (effectively another short-distance regularization) to define loops. Additionally, the enclosed area is not well-defined for loops that wind around the (periodic) lattice. We thus chose to exclude loops with non-zero winding number from consideration. Also, we note that these measured values presumably suffer from large systematic corrections because they do not satisfy the relation $\tau' = 1 + \delta'$, which can be derived through scaling arguments⁴. This relation also holds for the corresponding indices that describe the distribution of self-avoiding loops that bound clusters in the $2-d$ Ising model at the Curie temperature. In that case, $\tau' \sim 2.45$. Finally, we found that the scaling behavior of loops on slices slowly disappeared as we continued to increase the Ising temperature. At $\beta = .18$ on $L = 150$ SC lattices, we observed that very large loops were again exponentially suppressed in the distribution $N(l)$.

Should we be surprised by the presence of this ‘loop scaling’ at T_c ? The following argument, due to Antonio Coniglio, indicates that this result is at least plausible [24]. First, note that in the $T \rightarrow \infty$ limit, the distribution of loops and geometrical clusters is that of pure site percolation with $p = .5$. On the square lattice, $p_c \sim .59$ so that if only half the sites contain identical spins, then the distribution of loops and clusters should be governed by a finite correlation length. Now consider turning on the Ising couplings in the x and y directions. As the spins become correlated, the critical concentration⁵ needed for percolation should diminish. At the Curie temperature for the $2-d$ Ising model ($T_c^{d=2}$) this critical concentration decreases to $.5$ and geometrical clusters and their boundaries percolate. In two dimensions, this critical concentration cannot be less than $.5$, since generically two percolating clusters cannot span a single lattice [25]. Imagine next turning on the Ising coupling in the z direction while tuning the x and y couplings to remain at criticality. If the critical concentration remains $.5$ as the system reaches the

⁴We thank Bertrand Duplantier [23] for providing us with a derivation of this relation.

⁵Note that we can adjust the relative concentration of up and down spins by also adding a magnetic field.

3- d Curie temperature, then one would find a scaling distribution of clusters and boundaries on 2- d slices. On the other hand, we cannot rule out the possibility that the critical concentration again increases above .5; then we would never expect to find scaling of loops on slices of the 3- d Ising model.

We also observed scaling behavior of loops on the BCC lattice. In particular, only small loops were found at T_p while scaling of $N(l)$ with the values $\tau' = 2.23(1)$ and $\delta' = 1.23(1)$ occurred at T_c . The uncertainty in the value of T_c probably leads to a significant systematic error in the estimate of these exponents. They do obey the anticipated relation $\tau' = 1 + \delta'$; δ' is not particularly far from the estimate extracted from the SC data. Note that on slices of the BCC lattice, which are triangular, there is no longer any ambiguity in the definition of loops. In this case, $N(l)$ apparently satisfies a power-law distribution, with a temperature-dependent exponent, for all $T > T_c$! This observation can be fully understood theoretically, since the percolation threshold on triangulated lattices equals .5. Therefore, we definitely expect to observe loop scaling at $T = \infty$ with scaling exponents characteristic of 2- d percolation ($\tau' \sim 2.05$ and $\delta' = 1$). Since lowering the temperature increases correlations between spins, we expect to find percolated clusters on slices for all T . For $T < T_c$, however, minority spins cannot percolate on 2- d slices because, as stated above, only one infinite cluster can span a lattice. Thus the minority spins and the loops that enclose them must percolate at T_c on 2- d slices of the 3- d Ising model on the BCC lattice. If we assume that this phenomenon is independent of the particular lattice type, then it follows that loop scaling should always occur at T_c . A similar situation occurs for the 2- d Ising model on the triangular lattice: one can argue that the distribution $N(l)$ again scales as a power law for all $T > T_c$ because $p_c = 1/2$ on triangulated lattices.

It also seems reasonable that the presence of loop scaling may be related to the vanishing of the surface tension of the Ising model at T_c . The vanishing of the surface tension ensures that the free energy of a system with anti-periodic boundary conditions along one plane (essentially due the insertion of a large loop along the boundary) equals the free energy of a system with periodic boundary conditions.

We now comment on the significance of this scaling. As we noted in the previous two sub-sections, the geometrical cluster boundaries do not in the least resemble surfaces (in the continuum limit) at T_p . The presence of large loops at T_c might indicate that the boundaries grow large long handles.

A visual examination of successive slices qualitatively indicates that this is not so. Large loops seemingly always vanish after several consecutive slices. Indeed, it is difficult to envision a smooth surface that decomposes into a scaling distribution of loops along arbitrary slices.

It should also be noted that the exponent τ' is probably not directly related to the magnetic or thermal exponents of the $3-d$ Ising model. More generally, it may not be associated with the behavior of correlation functions of local operators in a unitary quantum field theory. This is true also for loops bounding clusters in the $2-d$ Ising model. For in all of these cases, the scaling of geometrical clusters is determined by the geometric effects associated with percolation as well as the long-range correlations due to Ising criticality. Still, this scaling law describes physics that in principle is observable, perhaps by counting domains in sections of crystals that lie in the universality class of $3-d$ Ising. It would thus be quite interesting to construct a theoretical scheme to compute (approximately) the value of τ' . These loops are significantly ‘rougher’ than the corresponding boundaries in the $2-d$ Ising model, since the exponent δ' is lower here. They gain more kinetic energy because they are given an extra dimension in which to vibrate; perhaps this is responsible for their increased roughness.

Ideally, we would like view these loops as string states that evolve in Euclidean time (perpendicular to the slices). Their dynamics is described by the transfer matrix determined from Boltzmann factors associated with their creation, destruction, merging and splitting. We have thus found that the ground state wave functional (string field) of this transfer matrix is peaked around configurations that describe a scaling distribution of loops. These loops seemingly bear little relation to free strings, though, because they interact strongly by splitting and joining every few lattice spacings⁶. One might hope that some sort of perturbative string description could still be viable if the strength of this interaction were just a short-distance artifact; i.e. if the string coupling diminished towards zero in the infrared. To gauge whether this is likely, we blocked spins in our simulations to measure the renormalization group flow of the operator that couples to the total Euler character summed over all cluster boundaries. In particular, during simulations on $L=128$ SC and BCC lattices, we blocked spins, using the majority rule and letting our random number generator decide ties. At each blocking

⁶In practice, this makes an analysis of the transfer matrix a formidable task.

lattice	128	64	32	16	8
BCC	.049 (3)	.039 (3)	.037 (3)	.039 (3)	.044 (3)
SC	.021 (2)	.020 (2)	.018 (2)	.015 (2)	.012 (1)

Table 1: The mean genus per lattice site at T_c for blockings ($L = 8, 16, 32$ and 64) of an $L = 128$ lattice.

level, we reconstructed clusters and boundaries and then measured the genus summed over surfaces. We present the results of this analysis in table 1; data was taken at $\beta_c = .221651$ on the SC lattice and $\beta_c = .0858$ on the BCC lattice.

The results are not so conclusive. In particular, since we lack a very precise determination of the Curie temperature on the BCC lattice, it is likely that by the final blocking the couplings have flowed significantly into either the high or low-temperature regimes. Thus, one should probably not take the increase in genus density in the final two blockings on the BCC lattice seriously. This effect is not a problem on the SC lattice, where we fortunately know the critical temperature (based on previous Monte Carlo Renormalization Group measurements) to very high accuracy. On the other hand, we suspect that the small L blocked values on the SC lattice may be unreliable, due to ambiguity in the definition of genus. We can at least infer that the genus density decreases a bit during the first few blockings, indicating that the coupling $\exp(-\kappa)$ does at least slowly diminish at the beginning of the RG flow. There is no clear indication, however, that the flow continues on to the weak string coupling regime. One might also object to our choice of blocking scheme. Indeed, perhaps it might be more appropriate to somehow block the cluster boundaries themselves rather than the spins. In practice this would probably be technically difficult.

5 Assessment

The prospects for passing from the Curie point to the regime in which surfaces are weakly coupled are addressed in the work of Huse and Leibler [5]. They qualitatively map out the phase diagram of a model of self-avoiding surfaces

with action (1). The large κ (large coupling to total Euler character) regime of their model lies in a droplet crystal phase, where the large percolated surface has shattered into a lattice of small disconnected spheres. Such a configuration maximizes the Euler density; it clearly does not correspond to a theory of surfaces. By estimating the free energy difference between phases, they argue that the transition to this droplet crystal is first order. Given this picture, there seems to be little evidence for the existence of a fixed point describing a weakly coupled theory of surfaces near the Curie point of the Ising model. Nevertheless, we cannot definitely exclude the possibility that there is still some path which we have not considered to a weak-coupling theory.

In conclusion, it appears that evidence of a continuum theory of surfaces has eluded us in our investigation of Ising cluster boundaries. We have found, however, that these cluster boundaries do exhibit an intriguing fractal structure that does not typically appear in models of lattice surfaces.

6 Acknowledgments

We would like to thank Stephen Shenker for essential discussions which led to our investigations. We also greatly benefitted from discussions and correspondence with Mark Bowick, Antonio Coniglio, Francois David, Bertrand Duplantier, John Marko and Jim Sethna. Furthermore, we are indebted to the organizers of this workshop for their efforts and hospitality. We are also grateful to NPAC for their crucial support. This work was supported in part by the Dept. of Energy grants DEFG02-90ER-40560, DEFG02-85ER-40231, the Mathematical Disciplines Institute of the Univ. of Chicago, funds from Syracuse Univ., by the Centre National de la Recherche Scientifique, by INFN and the EC Science grant SC1*0394.

References

- [*] Also at the Landau Institute for Theoretical Physics, Moscow
- [†] Laboratoire associé No. 280 au CNRS.
- [‡] Also at Dipartimento di Fisica and INFN, Università di Roma Tor Vergata, Viale della Ricerca Scientifica, 00133 Roma, Italy.
- [1] E. Fradkin, M. Srednicki and L. Susskind, Phys. Rev. **D21**, (1980) 2885; C. Itzykson, Nucl. Phys. **B210** (1982) 477; A. Casher, D. Føerster and P. Windey, Nucl. Phys. **B251** (1985) 29; Vl. Dotsenko and A. Polyakov, *in* Advanced Studies in Pure Math. **15** (1987).
- [2] E. Brézin and V.A. Kazakov, Phys. Lett. **236B** (1990) 144; M.R. Douglas and S.H. Shenker, Nucl. Phys. **B335** (1990) 635; D. J. Gross and A. A. Migdal, Phys. Rev. Lett. **64** (1990) 127.
- [3] G. Parisi, *in Proceedings of the Third Workshop on Current Problems in High Energy Particle Physics*, John Hopkins Conference, Florence 1979; G. Parisi, J.-M. Drouffe and N. Sourlas, Nucl. Phys. **B161** (1979) 397; B. Durhuus, J. Frohlich and T. Jonsson, Nucl. Phys. **B240** (1984) 453; J. Ambjorn, B. Durhuus, J. Frohlich and P. Orland, Nucl. Phys. **B270** (1986) 457; M. E. Cates, Europhys. Lett. **8** (1988) 719.
- [4] F. David, Europhys. Lett. **9** (1989) 575.
- [5] D. Huse and S. Leibler, J. de Physique **49** (1988) 605.
- [6] M. Karowski and H.J. Thun, Phys. Rev. Lett. **54** (1985) 2556; R. Schrader, J. Stat. Phys. **40** (1985) 533.
- [7] M. Caselle, F. Gliozzi and S. Vinti, Turin Univ. preprint DFTT-12-93.
- [8] F. David, Jerusalem Gravity (1990) 80.
- [9] D. Stauffer and A. Aharony, *Introduction to Percolation Theory*, (Taylor and Francis, London, U.K. 1992).
- [10] J. Cambier and M. Nauenberg, Phys. Rev. **B34** (1986) 8071.

- [11] C.M. Fortuin and P.W. Kasteleyn, *Physica* **57** (1972) 536.
- [12] A. Coniglio and W. Klein, *J. Phys.* **A13** (1980) 2775.
- [13] R.G. Edwards and A.D. Sokal, *Phys. Rev.* **D38** (1988) 2009.
- [14] C.-K. Hu, *Phys. Rev.* **B29** (1984) 5103.
- [15] J.-S. Wang, *Physica* **A161** (1989) 149.
- [16] R.H. Swendsen and J.-S. Wang, *Phys. Rev. Lett.* **58** (1987) 86.
- [17] V. Dotsenko, G. Harris, E. Marinari, E. Martinec, M. Picco and P. Windey, in preparation.
- [18] S. Kirkpatrick, in “Ill-Condensed Matter”, *Les Houches Proceedings*, Vol.31, ed. R. Balian, R. Maynard and G. Toulouse (North Holland, Amsterdam 1983) 372.
- [19] M. Hasenbusch and K. Pinn, *Munster Univ. preprint MS-TIP-92-24*.
- [20] V. Dotsenko, G. Harris, E. Marinari, E. Martinec, M. Picco and P. Windey, *Phys. Rev. Lett.* **71** (1993) 811.
- [21] C. Itzykson and J-M. Drouffe, *Statistical Field Theory*, Cambridge University Press, Cambridge (1989).
- [22] P.G. DeGennes, *La Recherche* **7** (1976) 919.
- [23] Bertrand Duplantier, private communication.
- [24] Antonio Coniglio, private communication.
- [25] A. Coniglio, C. Nappi, F. Peruggi and L. Russo, *J. Phys.* **A10** (1977) 205.

Figure Captions

Fig. 1 The Wigner–Seitz cell of the BCC lattice with next–nearest neighbor interactions.

Fig. 2 $\ln N(V_{cl})$ vs. $\ln V_{cl}$ for FK clusters on a $N = 64$ SC lattice.

Fig. 3 $\ln(V_{cl}/A_{cl})$ vs. $\ln V_{cl}$ for FK clusters on the $L = 64$ SC lattice.

Fig. 4 The number of genus 2 surfaces at T_c as a function of dual surface area A for FK clusters on the $L = 64$ BCC lattice, with a best fit to the functional form given in equation 5.

Fig. 5 As in the previous figure, but for genus 5.

Fig. 6 The dependence of μ (extracted from the moments of the area distribution) on genus for FK clusters on the $L = 64$ BCC lattice at T_c .

Fig. 7 The dependence of x (extracted from direct fits to (5) and moments) on genus for FK clusters on the $L = 64$ BCC lattice at T_c .

Fig. 8 The number of genus 1 surfaces at T_c as a function of dual surface area A for FK clusters on the $L = 64$ SC lattice, with a best fit to the functional form (5).

Fig. 9 As in the previous figure, but for genus 5.

Fig. 10 The number of genus 2 surfaces at T_p as a function of dual surface area A bounding minority (geometrical) clusters on the $L = 60$ BCC lattice.

Fig. 11 As in the previous figure, but for genus 5.

Fig. 12 The dependence of μ (extracted from moments) on genus for surfaces bounding minority (geometrical) clusters on the $L = 60$ BCC lattice at T_p .

Fig. 13 The dependence of x (extracted from fits and moments) on genus for surfaces bounding minority (geometrical) clusters on the $L = 60$ BCC lattice at T_p .

Fig. 14 A log–log plot of the distribution of loops of length l on slices of an $L = 60$ SC lattice at T_p .

Fig. 15 A log–log plot of the distribution of loops of length l on slices of an $L = 150$ SC lattice at T_c .

This figure "fig1-1.png" is available in "png" format from:

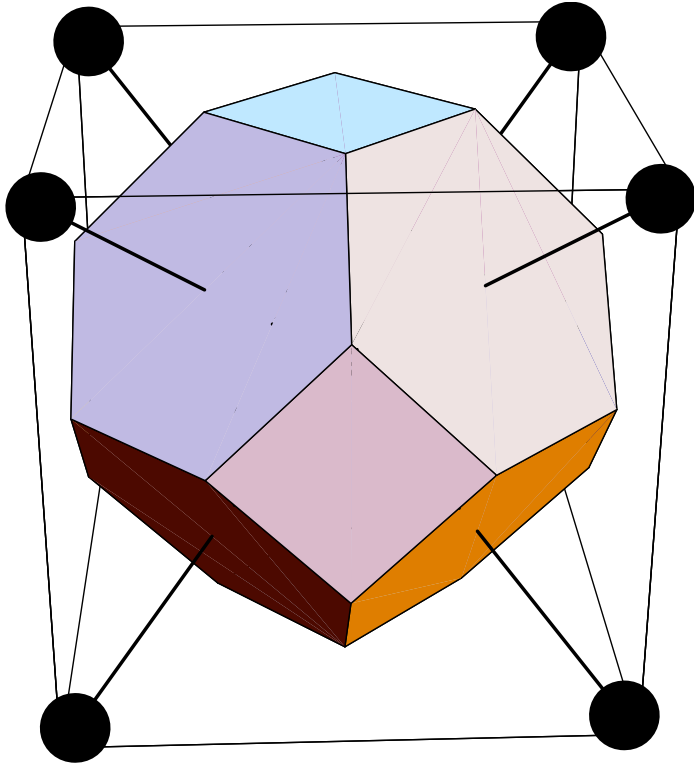
<http://arxiv.org/ps/hep-th/9401129v1>

This figure "fig2-1.png" is available in "png" format from:

<http://arxiv.org/ps/hep-th/9401129v1>

This figure "fig3-1.png" is available in "png" format from:

<http://arxiv.org/ps/hep-th/9401129v1>



This figure "fig1-2.png" is available in "png" format from:

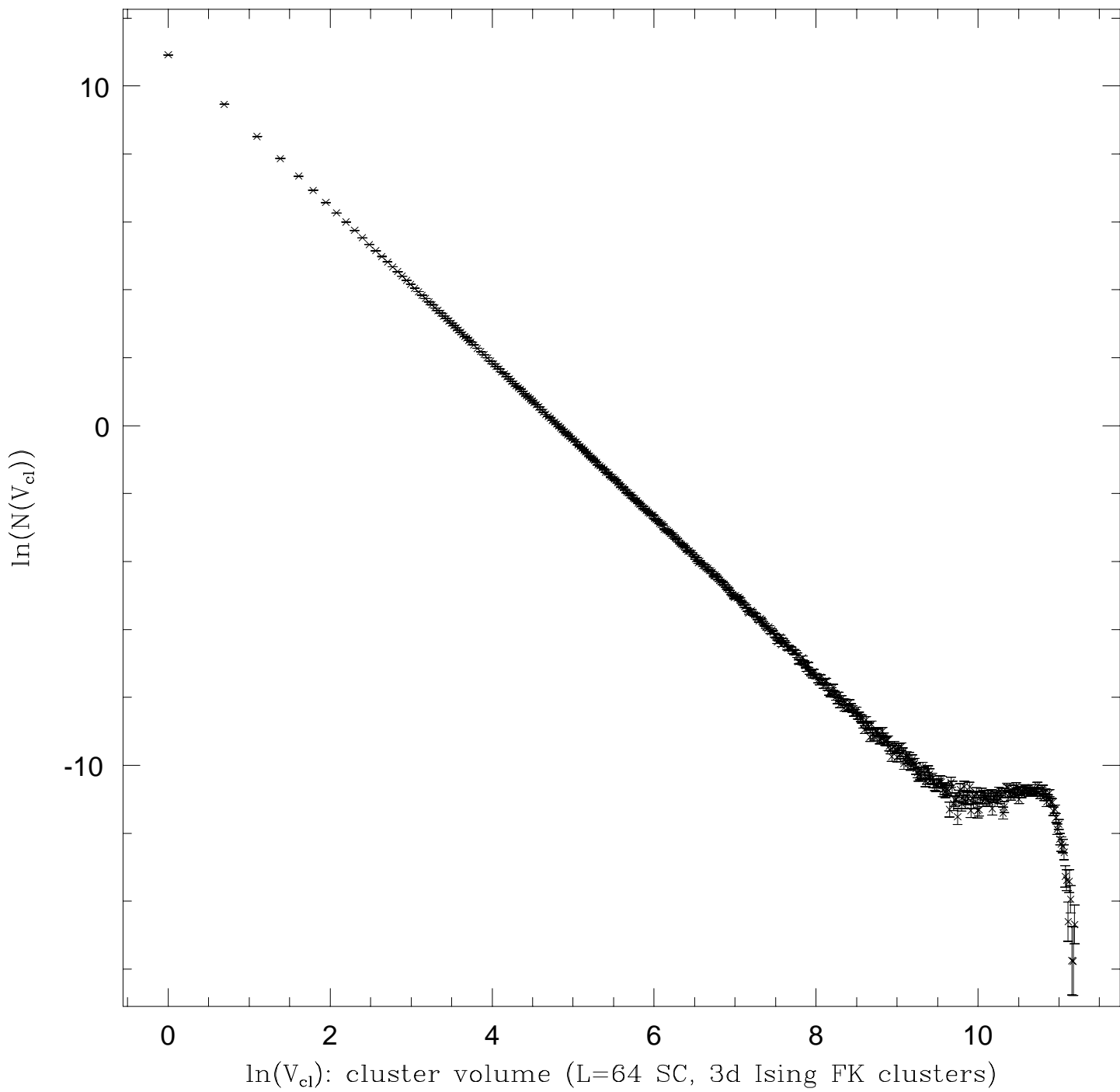
<http://arxiv.org/ps/hep-th/9401129v1>

This figure "fig2-2.png" is available in "png" format from:

<http://arxiv.org/ps/hep-th/9401129v1>

This figure "fig3-2.png" is available in "png" format from:

<http://arxiv.org/ps/hep-th/9401129v1>



This figure "fig1-3.png" is available in "png" format from:

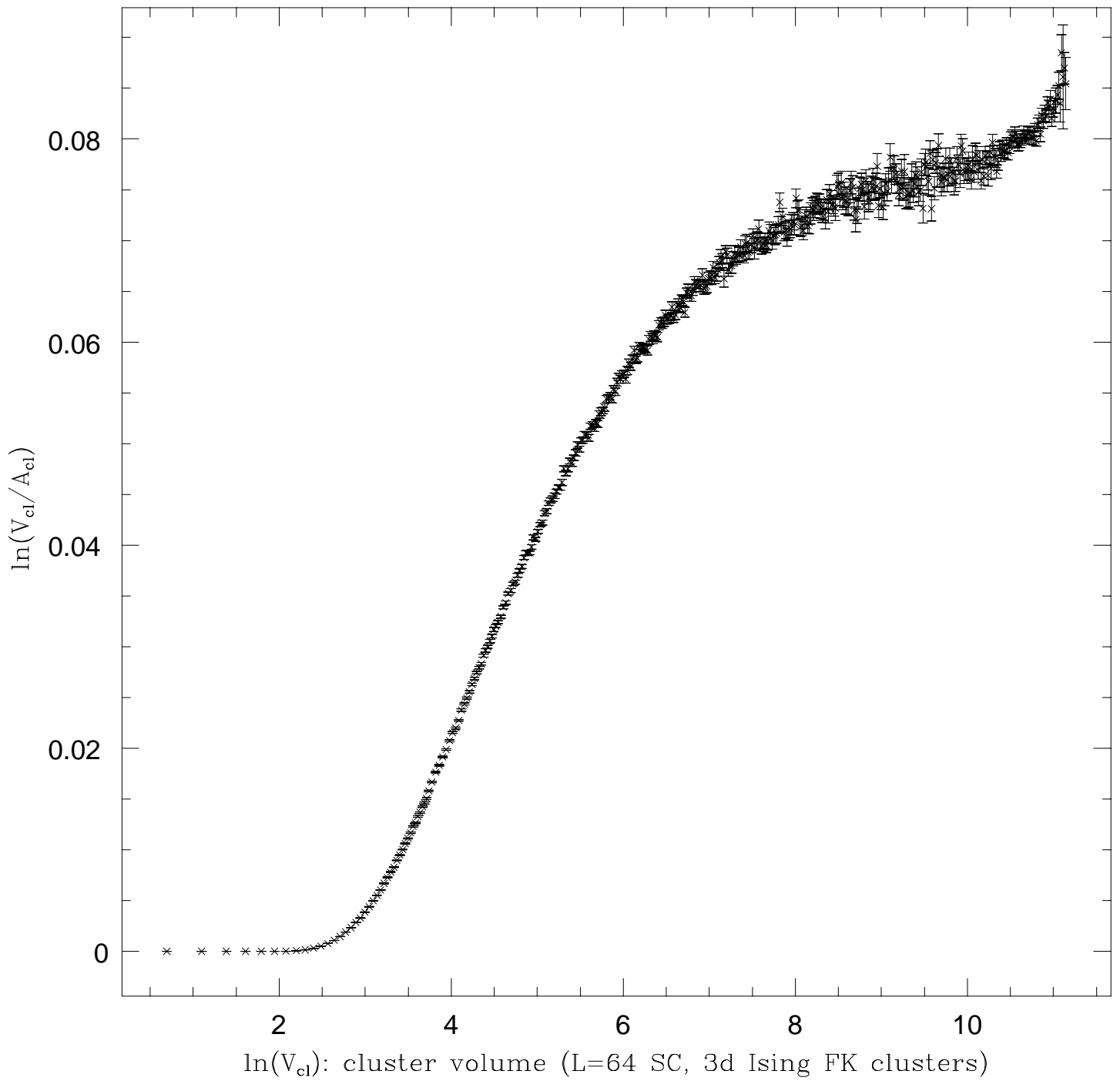
<http://arxiv.org/ps/hep-th/9401129v1>

This figure "fig2-3.png" is available in "png" format from:

<http://arxiv.org/ps/hep-th/9401129v1>

This figure "fig3-3.png" is available in "png" format from:

<http://arxiv.org/ps/hep-th/9401129v1>



This figure "fig1-4.png" is available in "png" format from:

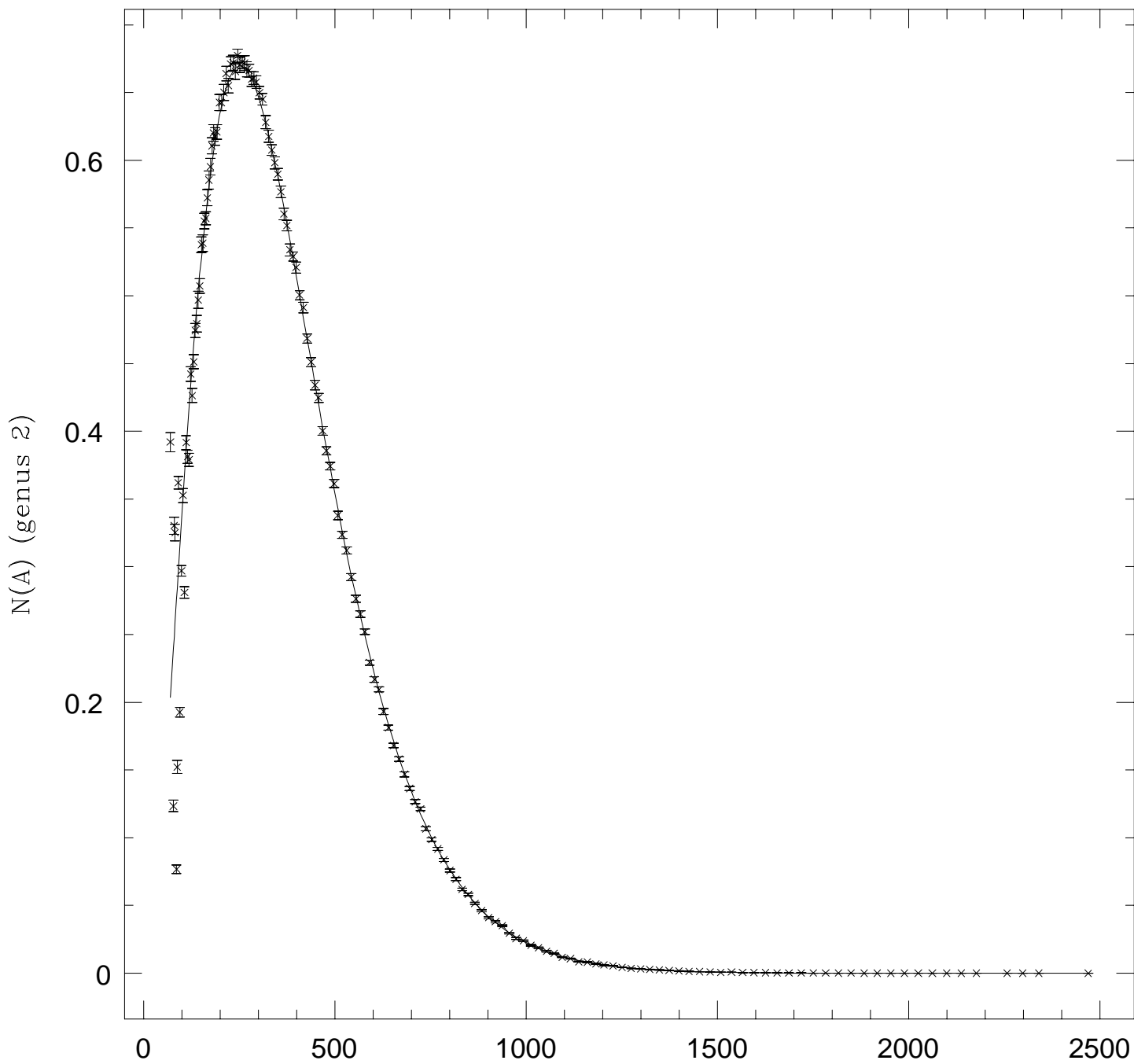
<http://arxiv.org/ps/hep-th/9401129v1>

This figure "fig2-4.png" is available in "png" format from:

<http://arxiv.org/ps/hep-th/9401129v1>

This figure "fig3-4.png" is available in "png" format from:

<http://arxiv.org/ps/hep-th/9401129v1>



A: Dual Surface Area (L=64 BCC, 3d Ising FK clusters)

This figure "fig1-5.png" is available in "png" format from:

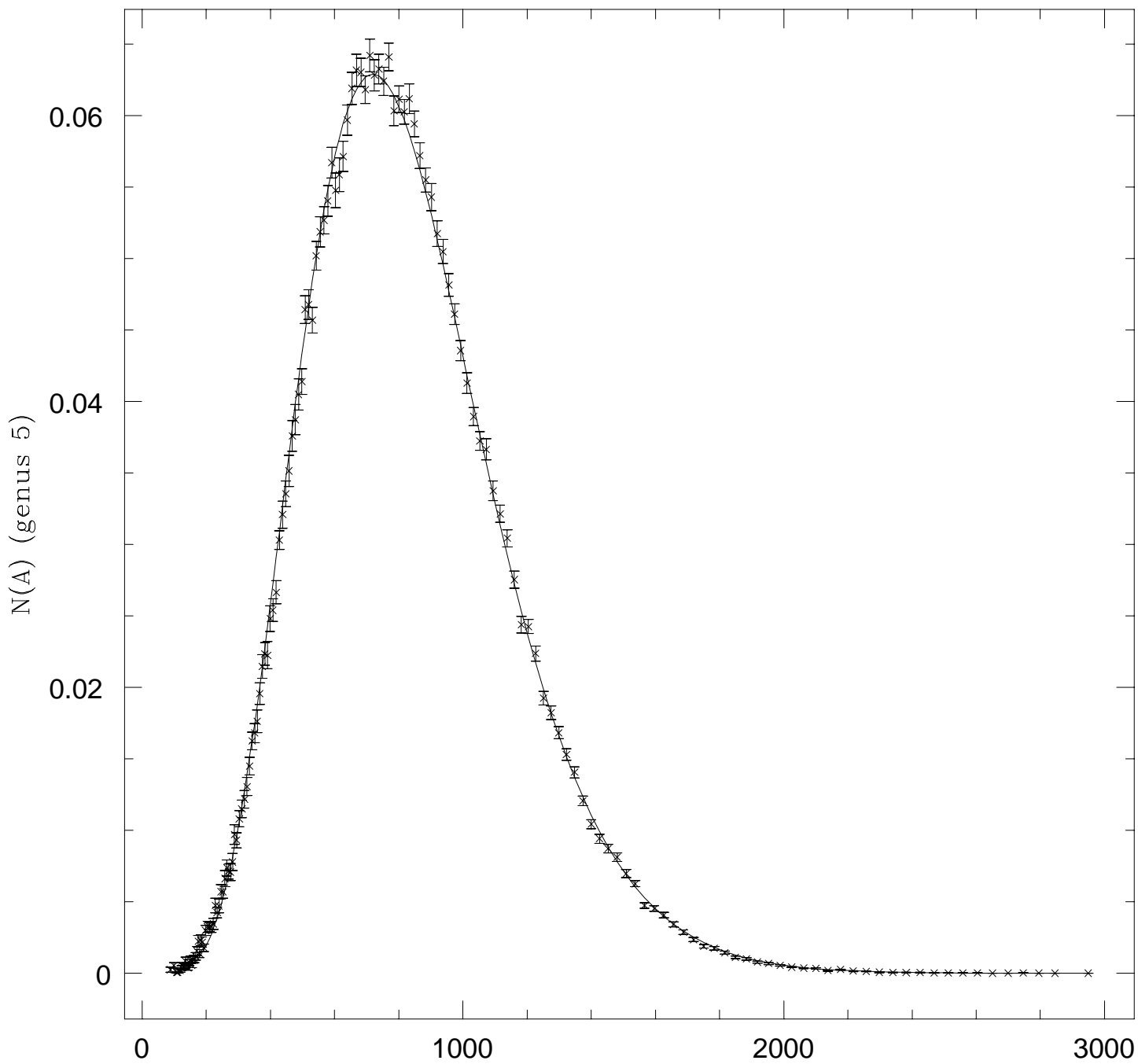
<http://arxiv.org/ps/hep-th/9401129v1>

This figure "fig2-5.png" is available in "png" format from:

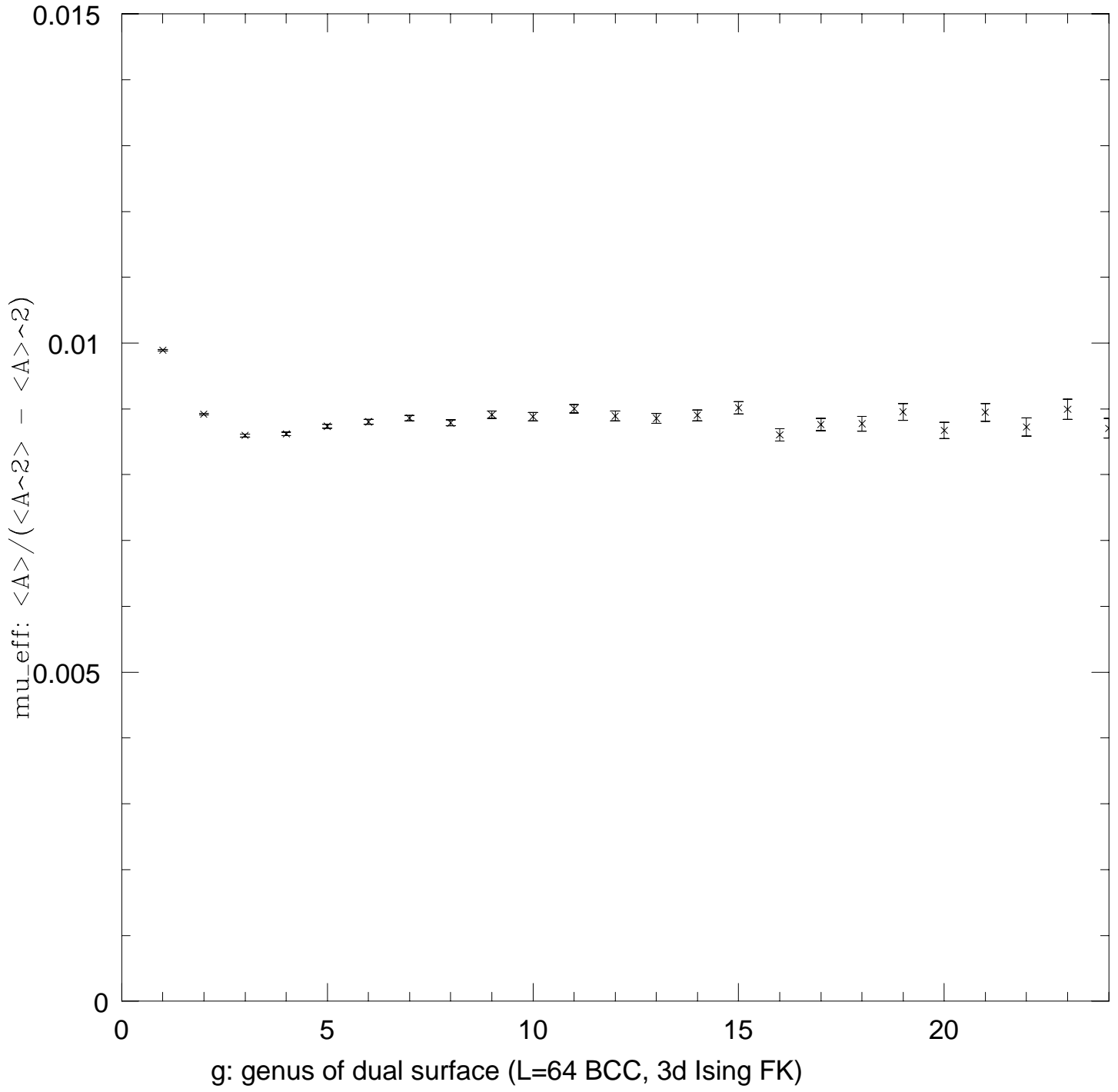
<http://arxiv.org/ps/hep-th/9401129v1>

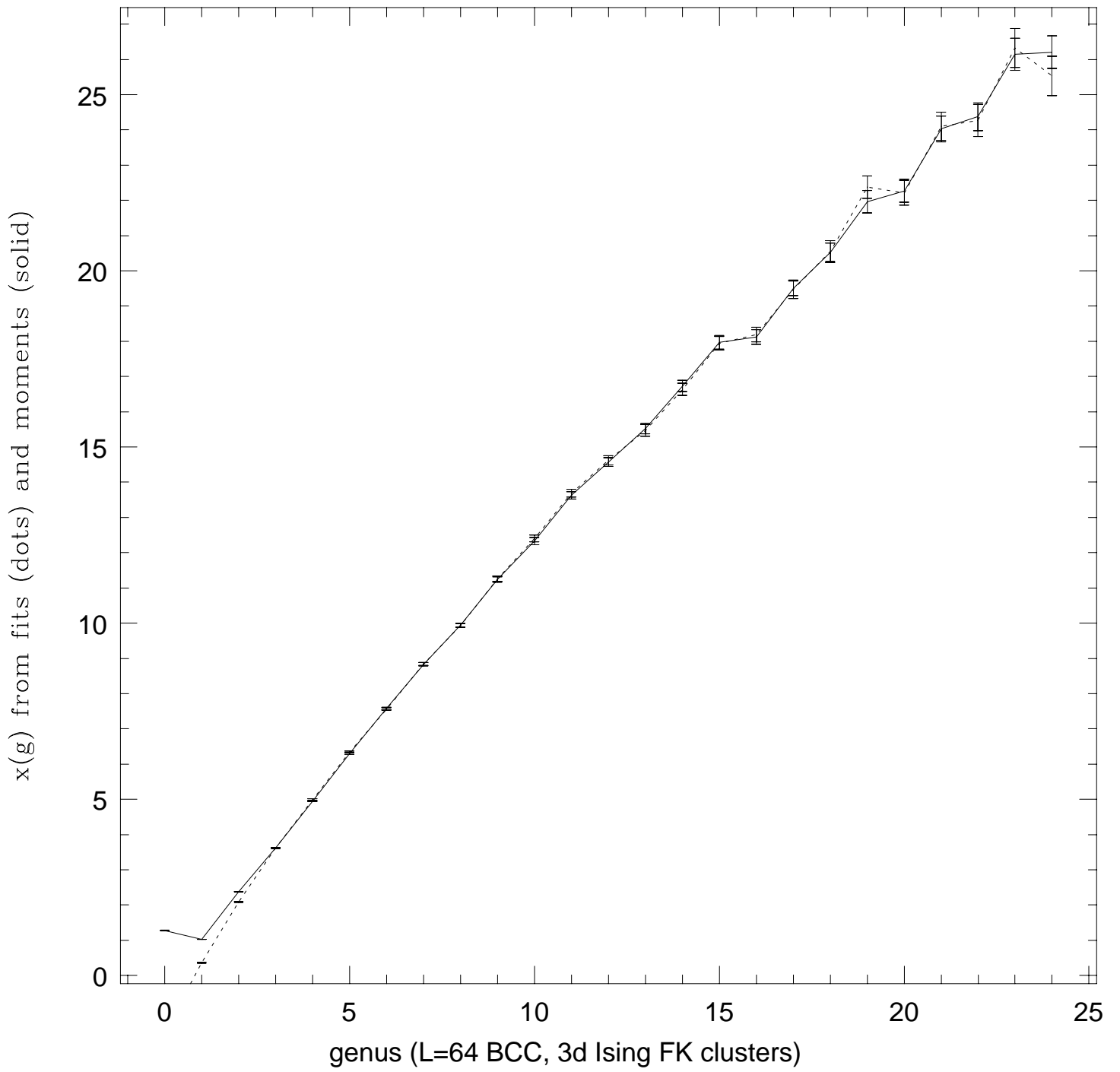
This figure "fig3-5.png" is available in "png" format from:

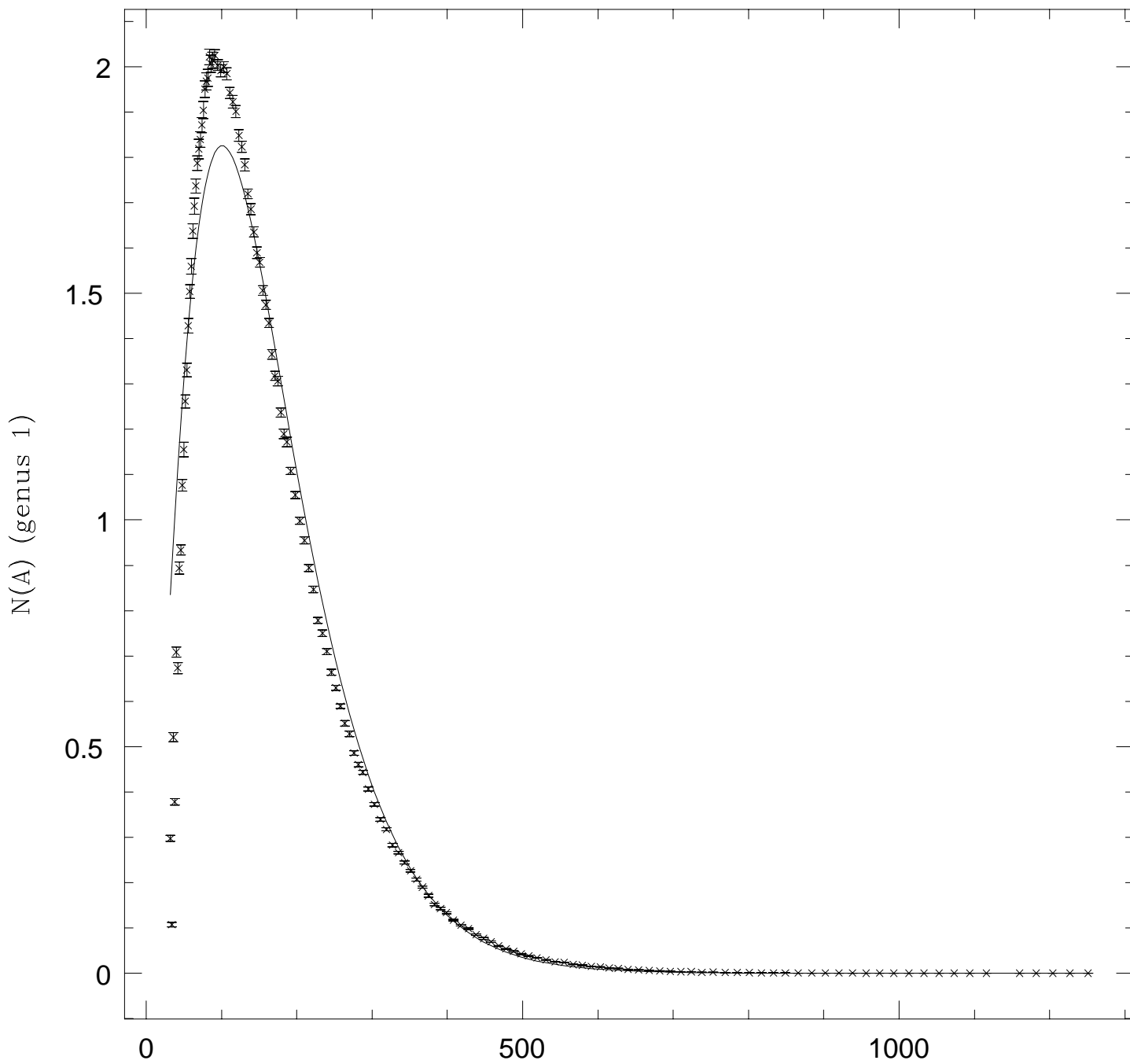
<http://arxiv.org/ps/hep-th/9401129v1>



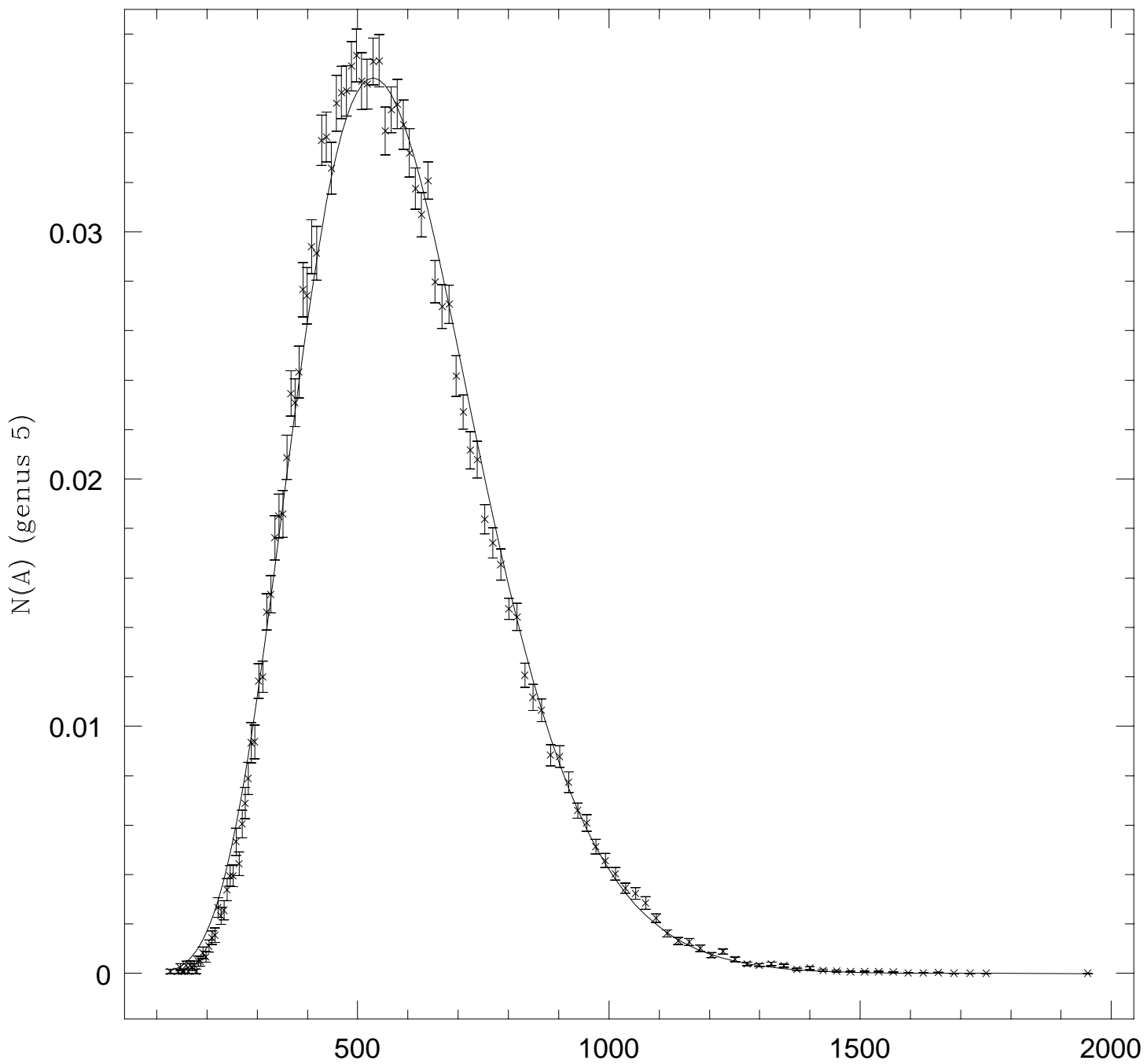
A: Dual Surface Area (L=64 BCC, 3d Ising FK clusters)







A: Dual Surface Area (L=64 SC, 3d Ising FK clusters)



A: Dual Surface Area (L=64 SC, 3d Ising FK clusters)

